Engineered Science
DOI : https://dx.doi.org/10.30919/es1156

Design and Manufacturing With 3D Printing and Life Cycle Analysis of a Recyclable Polymer-Based H-Darrieus Wind Turbine

Andrés F Olivera,[1, 2] Edwin Chica,[2,*] and Henry A Colorado[1,*]

Abstract

Additive manufacturing (AM), also known as 3D printing (3DP) has revolutionized the development of components with complex shapes, enabling better developed surfaces, favoring aerodynamic shapes, using moldable and easy-to-reuse materials for aerodynamics; and involving hydrodynamics, energy, and transportation industries. One industry that has benefited from this progress is wind energy. In this research, a small-scale H-Darrieus type wind turbine is designed to be manufactured by a 3D printer, using a filament of polyethylene glycol terephthalate (PETG) with carbon fiber. The turbine was made at laboratory scale with a height and diameter of 0.20 m and 0.22 m, respectively. This model was tested later in a wind tunnel. The maximum power coefficient obtained was 0.21 at a tip speed ratio (TSR) of 0.12. The life cycle of the turbine was analyzed considering manufacturing process, operation, and its disassembly to be recycled or reused. Results show the manufacturing of H-Darrieus turbines is a sustainable solution for the environment and communities. This research shows innovative results in the design, materials, and environmental impact calculations of a low scale wind turbine.

Keywords: H-Darrieus turbine; Thermoplastic recycling; Blade recycling; Circular economy; 3D printing.
Received: 12 February 2024; Revised: 12 March 2024; Accepted: 20 March 2024.
Article type: Research article.

1. Introduction

During the last decades, the use of polymeric materials in various applications has increased significantly because of the advantages that include ease of processing, relatively high strength, low density and weight, and low cost.[1]

Multiple thermoplastic materials show superior properties[1,2] making them very common in the aerospace, automotive, and wind power industries.[3,2]

Some of the materials used for the manufacture of blades include polymeric resins, the most widely used material for the manufacture of wind turbine blades.[4] The thermoplastic polymers show also advantages over the thermosets, such as a higher fracture toughness. Polymeric resins (thermosets) are more used in composite industries due to their low viscosity and simple processing when compared to thermoplastics.[5] Thermosets are also used because they can be cured at low or room temperatures, and with their lower viscosity, the process is facilitated. Initially, polyester resins were extensively used in this sector, but with the development of large wind turbines, epoxy resins substituted them.[5,6]

On the other hand, thermoplastics show much better recyclability than thermosets. However, they require high processing temperatures, increasing energy consumption and difficulties in the manufacturing of large surfaces (more than 2 m in length), due to their much higher viscosity.[7] Although the fracture toughness of thermoplastics is higher than that of thermosets, the fatigue behavior of thermoplastics is generally lower than for thermosets, even for composites with carbon or glass fibers reinforcements.[6,5,4]

With respect to the fiber reinforcements, when the E glass fibers contents increases (or borosilicate glass due to its good electrical resistance), stiffness, tensile, and compressive strength increases proportionally.[8,9] However, at a high fiber

[1] *CCComposites, Facultad de ingeniería, Universidad de Antioquia, Calle 70 No. 52-21, Medellín 050010, Colombia.*
[2] *Grupo de Energía Alternativa, Departamento de ingeniería Mecánica, Facultad de Ingeniería, Universidad de Antioquia, Calle 70 No 52-21, Medellín 050010, Colombia.*
**Email:* edwin.chica@udea.edu.co (E. Chica), henry.colorado@udea.edu.co (H. A. Colorado)

volume content over 65%, a lack of resin probably due to agglomeration is observed, causing that the fatigue strength of the compound is reduced. The epoxy/glass fiber composites for wind blades typically contains up to 75 wt% of glass fibers.[8,9]

Carbon fibers present a good alternative to glass fibers due to their superior stiffness and lower density. This characteristic enables the creation of thinner, stiffer, and lighter blades. However, it is important to note that carbon fibers exhibit lower damage tolerance, compressive strength, and relatively limited maximum strain when compared to glass fibers. Additionally, carbon fibers are considerably more expensive than E-glass fibers.[8-10] Carbon fiber reinforced composites are sensitive to misalignment and fiber curl: small misalignments lead to strong compression reduction and fatigue resistance. The utilization of carbon fiber composites is widespread in the production of large wind turbine blades, with notable companies such as Vestas, headquartered in Aarhus, Denmark, and Siemens Gamesa, based in Zamudio, Spain.[11]

Aramid fibers are a feasible alternative material as well, also called aromatic polyamide, which demonstrate high mechanical strength, high toughness, and damage tolerance. However, they show low compressive strength, low adhesion to polymeric resins, high moisture absorption, and degradation due to ultraviolet radiation.[12]

Basalt fibers are another feasible option, with good mechanical properties: 30% stronger, 15–20% stiffer, 8–10% lighter than E-glass fibers; while they are cheaper than carbon fibers.[13] Basalt fibers has been used by Mengal *et al*., where a basalt-carbon hybrid composite was used to produce blades wind turbines.[14] Chikhradze *et al*. used fiber-reinforced hybrid composites and basalt nanopowders for wind turbines, obtaining important results.[15] In terms of the scale, the world's longest wind turbine rotor blade currently measures 118 m long, led by Mingyang Smart Energy company, made from carbon fiber composites.[16]

Natural fibers such as sisal, flax, hemp, and jute, offer compelling alternatives owing to their numerous advantages: affordability, widespread availability, and environmentally friendly attributes. The disadvantages are a high variability in properties, high moisture absorption, and a low thermal stability of raw fibers.[17,18] Piggot *et al*. tested a novel epoxy laminated bamboo and poplar for wind turbine blades, showing high strength and stiffness to be used on wind blades. The high strength and durability of bamboo, as well as its rapid growth make bamboo a promising wind material for energy applications.[19]

Regarding the typical manufacture of wind turbines for horizontal HAWT (Horizontal axis wind turbine) turbines, they are made from prefabricated molds, where two shells are generated using resins and fibers. These reinforcements are normally made with 75wt% glass fiber and 25wt% epoxy or polyester resins, arranged in layers, then processed by vacuum to remove air bubbles. Once the two sections are obtained, they are bonded using an epoxy adhesive joint. In the center of these components, a mast is strategically positioned to serve as a central column, tasked with efficiently bearing the wind loads. It undergoes a crucial treatment process wherein it is coated with specialized protective paints. These coatings serve a dual purpose: firstly, they shield the mast from the adverse effects of weather conditions, such as corrosion and degradation caused by exposure to sunlight, moisture, and temperature variations. Secondly, certain types of paints are designed with conductive properties, which can help to dissipate electrical charges, thereby reducing the likelihood of lightning strikes. This preventive measure is particularly important in regions prone to thunderstorms or areas where lightning poses a significant risk to the structural integrity of wind turbine components.[20]

For some vertical VAWT (Vertical axis wind turbine) turbines, there are manufacturing processes that can be much simpler than for HAWT horizontal turbines. This is because the aerodynamic profile can be made uniform throughout the length of the blade, as long as when the design of their blades is straight, a blade that can be developed by extrusion of an aluminum alloy with a low cost in labor and material costs. This technique is applicable to polymers reinforced with glass or carbon fibers for the manufacture of blades in VAWT turbines.[21,22]

The 3D prototyping has been used in the green energy sector to produce aerodynamic research models,[23,24] hydro turbine prototypes[25] and, recently, micro-scale wind turbines.[26] With the advent of affordable and accessible 3D technology, there is an opportunity for the wind power industry to take an approach to small wind turbine design. These can be made in a modular way to facilitate their fabrication, transport, and installation. Additive manufacturing through fused deposition modeling (FDM) was used to make wind turbines, particularly for testing certain component properties within a controlled environment before sending a design into production. Manufacturing low-ladder wind turbines can bring benefits to the end user, as they can get a low-cost turbine with considerable energy savings. These manufacturing processes facilitate the accessibility of wind turbines worldwide.[27-29] Rural electrification projects where wind power can be used to provide basic electricity could benefit from this technology. These wind turbines can be manufactured on site. Due to the low cost of filament material,

printers are available for values between $200 and $800 USD for basic printers, which suggest that wind turbines can be made at very reduced cost.[27-30]

The current research shows the design of a low-power H-Darrieus type wind turbine on a laboratory scale, beginning with the selection of the chord width according to the dimension's limitations by 3D printing apparatus. The aerodynamic profile to be used for this case was NACA 0024. This turbine is exposed to environmental conditions in a wind tunnel, which allows to obtain, through a sensor, the torque and the rotation speed. Through this data was obtained the electrical power delivered by the turbine, which was 0.52 w, when the air speed was 6 m/s and the generator rotated at 198 RPM. The life cycle of the blades was analyzed to verify if the recyclable manufacturing material can be reused after dismantling.

2. Methods and materials

2.1 Design methodology

The aerodynamic analysis quantifies the kinetic energy of the air that can be transferred to the wind turbine.[31] For this, the actuator disk model[32,33] is used, where the turbine is represented by a circular disk through which the air current flows with a speed $W_{-\infty}$, this movement of the air generates a pressure drop p , in the intermediate position of the actuator disc, as shown in Fig. 1. For the actuator disk model is assumed that there is no resistance to friction, therefore the flow is in a plane, homogeneous, and incompressible state. A control volume is also assumed, in which the boundaries are surfaces with two tube-shaped cross sections. To analyze this control volume, four regions are considered. The first is free flow region; the second is just before the blades; the third just after the blades: and the last the fourth region is the stela.[34]

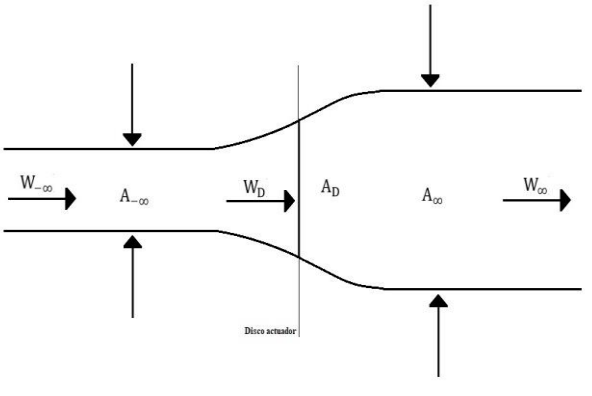

Fig. 1 Actuating disk in a flow tube.

Figure 1 shows a flow tube which does not have a constant area because the disc extracts part of the energy from the wind, and thus, the speed of the fluid decreases. To ensure that the continuity equation holds as one variable decreases, the other must increase. As the wind speed decreases, the area must increase, in this way it is established in Eq. (1) that:

$$\rho A_{-\infty} W_{-\infty} = \rho A_D W_D = \rho A_{\infty} W_{\infty} \quad (1)$$

where (ρ) is the air density, (A) is the cross-sectional area and (W) is the wind speed. In the same way, the amount of movement (M) that delivers an air mass m to the actuator disc can be determined by Eq. (2).[34]

$$M = m(W_{-\infty} - W_{\infty}) \quad (2)$$

While the forces (F) that interact between the air flow and the actuator disc are governed by Newton's second law, which can be expressed by Eq. (3).[34]

$$F = \frac{dM}{dt} = \dot{m}\,(W_{-\infty} - W_{\infty}) = \rho_w A_D W_D (W_{-\infty} - W_{\infty}) \quad (3)$$

The kinetic energy (E_c) delivered by the air mass is governed by Eq. (4).

$$E_c = \frac{1}{2} m (W_{-\infty}^2 - W_{\infty}^2) \quad (4)$$

And the power delivered by the air (P_w) to the actuator disc can be determined by Eq. (5).[34]

$$P_w = \frac{1}{2}\,\rho A_D W_D (W_{-\infty}^2 - W_{\infty}^2) \quad (5)$$

The power finally extracted by the actuator disc (P_D) will be given by Eq. (6)[34]

$$P_D = F W_D = \frac{1}{2}\,\rho A_D W_{-\infty}^3 C_P \quad (6)$$

where (C_P) is the power coefficient of the actuator disc, which can be determined from Eq. (7).

$$C_P = \frac{P_D}{P_w} \quad (7)$$

If we substitute Eqs. (5) and (6) in (7), we would have the power coefficient of the disc given by Eq. (8).[34]

$$C_P = \frac{\frac{1}{2}\rho A_D W_{-\infty}^3 4a(1-a)^2}{\frac{1}{2}\rho A_D W_{-\infty}^3} = 4a(1-a)^2 \quad (8)$$

Therefore, the power of the disc will be governed by Eq. (9).

$$P_D = \frac{1}{2}\,\rho A_D W_{-\infty}^3 4a(1-a)^2 \quad (9)$$

where a is given in Eq. (10):

$$a = 1 - \frac{W_D}{W_{-\infty}} \quad (10)$$

Being (a) the flow factor; from Eq. (8) it can be deduced that C_P Maximum is (16)/27=0.593, which is demonstrated by tabulating values of a between (0.1 and 1) with intervals of 0.05.[35] Therefore, Fig. 2 is obtained.[34]

With a value of the flow factor a=1/3, the maximum power coefficient would be 59.3%, which reflects what is known as the Betz limit and it is due to the impossibility to extract 100% of the kinetic energy of the wind since this would imply that the final speed of the wind was zero, that is, no flow.[35]

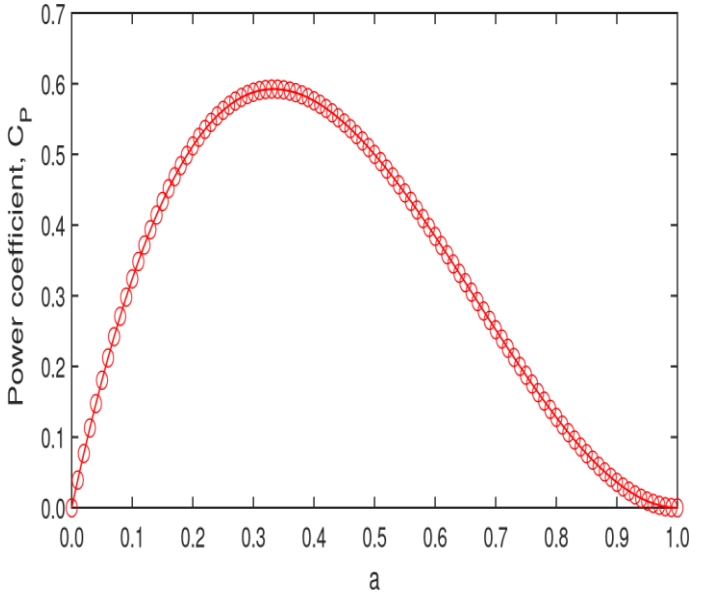

Fig. 2 Obtaining the maximum power coefficient vs. the flow factor.

Additionally, this value only happens when we have a constant linear flow, not viscous and not turbulent. If on the contrary it happens, detaching from vortices or wake rotation, the efficiency will be further reduced.

An efficiency factor for mechanical and electrical losses (η) equivalent to 0.75 must be added to Eq. (9). This is because the system, when it transforms mechanical energy into electrical energy, has an energy loss, which could be loss in the form of heat by the conducting cables. In this way, the final power equation obtained by the wind turbine is obtained given in Eq. (11), as (P_t):

$$P_t = \frac{1}{2}\,\rho A_D W_{-\infty}^3 C_P \eta \tag{11}$$

A_D is defined as the area that surrounds the blades in their movements and is related to the rotor diameter (D) and the blade height (H). The area is defined by Eq. (12).

$$A_D = DH = 2R \tag{12}$$

On the other hand, the tip speed of the blade or TSR (λ) directly affects the power coefficient and is defined by Eq. (13).[34]

$$\text{TSR}\ (\lambda) = \frac{R\psi}{W_{-\infty}} \tag{13}$$

where (ψ) is the rotational speed of the turbine. The TSR value relates the tangential velocity at the tip of the blade and the air velocity.[36] Each wind turbine configuration is different, which produces a different C_P for each one. There are low speed turbines such as Savonious rotors or Multiblade mills which have low efficiency. Likewise, there are horizontal rotors with 1, 2, and 3 blades Darrieus rotors with much higher C_P,[37,38] giving a greater efficiency in the ranges between 35 and 50%.[37] The higher the TSR, the aerodynamic profile should be more close to the optimal, since turbines with very high speeds tend to decrease their efficiency.[37]

On the other hand, there is a shape factor (A_DR) that relates the height of the blade (H) and the radius of the turbine (R). This factor can oscillate between 1 and 4 for vertical axis wind turbines. In this research, the relationship of 2 was used, represented by Eq. (14)[39,37,34]

$$A_D R = \frac{H}{R} \tag{14}$$

For the design of the blades, the chord length (c) could be obtained by equating the turbine thrust (I), given by the actuator disc theory, and with the turbine thrust given by the theory moment in the blade, see Eq. (15).[37,34]

$$I = 2\rho A_D a(1-a) W_{-\infty}{}^2 \tag{15}$$

The forces that interact in a vertical axis turbine can be interpreted by means of the blade element theory and the moment at the turbine.[40] The forces act during the entire revolution of the blade. There is a component of lift force F_L in the direction of rotation, while the moment produced varies with respect to the position of the blade.[35] The smaller the number of blades, the greater the number of blades will be variation in torque.[36] The angle of attack (α) in this vertical axis turbine varies as a function of the azimuth angle (θ). It is also possible to show that the rotation of the turbine is produced by F_L and the velocity vector ($W_{-\infty}$)), or (W) breaks down into a normal vector (F_N) and a tangential vector (F_T) giving rise to the following Eq. (16).[41,42]

$$w = \sqrt{(v_i \sin(\theta))^2 + (v_i \cos(\theta) + \psi R)^2} \tag{16}$$

where v_i is the velocity through the turbine; w can be expressed in a dimensionless way using the speed of the free current, in Eq. (17).[34]

$$\frac{w}{W} = \sqrt{\left(\frac{v_i}{W}\sin(\theta)\right)^2 + \left(\frac{v_i}{W}\cos(\theta) + \frac{\psi R}{W}\right)^2} \tag{17}$$

v_i can be rewritten in terms of a.

$$v_i = V(1-a) \tag{18}$$

With Eqs. (14) and (18), we substitute in Eq. (16) and obtain[34]

$$\frac{w}{W} = \sqrt{\left((1-a)\sin(\theta)\right)^2 + \left((1-a)\cos(\theta) + \lambda\right)^2} \tag{19}$$

In addition we can say that:

$$w = \frac{v_i \text{Sin}(\theta)}{\text{Sin}(\alpha)} \tag{20}$$

$$w = \frac{W(1-a)\text{Sin}(\theta)}{\text{Sin}(\alpha)} \tag{21}$$

The angle of attack (α) can be expressed as a function of Eq. (22)[34]

$$\tan(\alpha) = \frac{v_i \text{Sin}(\theta)}{v_i \cos(\theta) + \psi R} \tag{22}$$

Eq. (22) can be expressed in a dimensionless way using Eq. (18).[34]

$$\alpha = \tan^{-1}\left(\frac{(1-a)\mathrm{Sin}(\theta)}{(1-a)\cos(\theta)+\lambda}\right) \quad (23)$$

As shown in Eq. (23), the angle of attack is affected by the azimuth angle (θ). This variation in the position of the blade produces a variation in the torque. It can also be seen that the fewer the number of blades, the oscillation of the torque will be greater.

The normal and tangential force of the blade can be expressed as follows[34]

$$F_N = \frac{1}{2}\rho w^2 Hc\left(C_L\mathrm{Cos}(\alpha) + C_D\mathrm{Sin}(\alpha)\right) \quad (24)$$

$$F_T = \frac{1}{2}\rho w^2 Hc\left(C_L\mathrm{Sin}(\alpha) - C_D\mathrm{Cos}(\alpha)\right) \quad (25)$$

where (C_L) is the lift coefficient and (C_D) is the drag coefficient. The instantaneous buoyant force of the air (I_i) on the turbine can be expressed as follows[34]

$$I_i = F_N\mathrm{Sin}(\theta) - F_T\mathrm{Cos}(\theta) \quad (26)$$

Eqs. (24) and (25) are replaced in Eq. (26), obtaining[34]

$$I_i = \frac{1}{2}\rho w^2 Hc\left[\left(C_L\mathrm{Cos}(\alpha) + C_D\mathrm{Sin}(\alpha)\right)\mathrm{Sin}(\theta) - \left(C_L\mathrm{Sin}(\alpha) - C_D\mathrm{Cos}(\alpha)\right)\mathrm{Cos}(\theta)\right] \quad (27)$$

This is how from Eq. (11), (19) and (25), (c) can be found:[34]

$$c = \frac{8aR\mathrm{Sin}^2(\alpha)}{(1-a)\mathrm{Sin}^2\theta\left(C_D\mathrm{Cos}(\alpha-\theta) - C_L\mathrm{Sin}(\alpha-\theta)\right)} \quad (28)$$

According to Eq. (26), the azimuth angle (θ) values are from 0° to 360°. The angle of attack (α) is kept fixed at 5° to guarantee good aerodynamic performance. In the same way, for each aerodynamic profile, a value of (C_L) and (C_D) defines the profile to be used in the turbine will be NACA 0024.[43] It was found in the literature that the values of lift and drag coefficient for an angle of attack of 5° will be 0.8435 and 0.05489 respectively, while the axial induction factor value is 0.76. The value of R is 0.11.[34,43]

Analyzing Fig. 3 only were shown azimuth angle values between 60 and 120°, since significant chord length values are obtained in this range. Values below 50° and above 130° are neglected as they do not show values that might be too large for chord length. The wind turbine to be developed will be designed on a laboratory scale, for which must be taken into account the following parameters: density of the air of 1.2 Kg/m^3, area of the turbine for which the height of the blade of 0.2 m, and radius of the turbine of 0.11 m, parameters all designated to determine the average speed of the air in Medellín, the city where the turbine will be installed. The atlas is taken as a reference of the wind and wind energy of Colombia, carried out by the energy mining planning unit (UPME), attached to the Colombian Ministry of Mines and Energy.[34,44,45] The average map shows in the Antioquia region average annual speeds between 2 and 3.5 m/s, therefore setting a value of 2.5 m/s. The power coefficient will be 0.25[40] and the efficiency in the generation and transformation of energy will be 0.75. By assuming a fixed value of (α), (C_L) and (C_D), which represent the best performance of the turbine, a value of chord length c = 29.4 mm is obtained, specifically by averaging the values in Fig. 3, with Azimuth Angle between 60 and 120°. The summary of all these parameters is presented in Table 1, while the blade profile can be seen in Fig. 4.

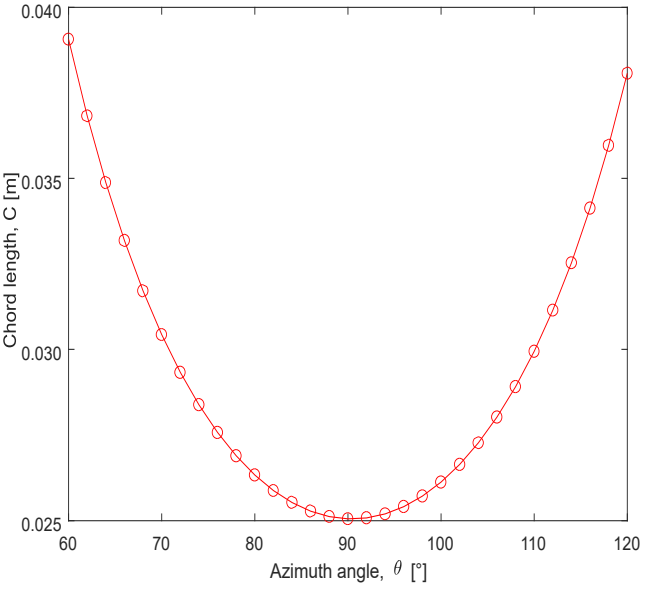

Fig. 3 Chord length (mm) vs Azimuth angle.

Table 1. Parameters for the design of the H-Darrieus wind turbine with NACA 0024 profile.

Design parameter	Value
Air Density (kg/m^3)	1.2
Turbine área (m2)	0.044
Blade height (m)	0.2
Turbine radius (m)	0.11
Estimated air speed (m/s)	2.5
Power Coefficient (C_P)	0.3
Mechanical and electrical efficiency (η)	0.75
Blade airfoil	NACA 0024
Chord length (mm)	29.4

The non-dimensional coordinates for the NACA 0024 profile are obtained from air foil tools.[46] These dimensionless measurements are multiplied by the length of the chord, generating the profile shown in Fig. 4a. Thus, the aerodynamic profile is obtained, necessary to obtain the design of the blades, shown in Fig. 4b, which illustrates the blade with a chord length of 29.4 mm and a length of 210 mm, plus adding 5 mm to each support disk. In the same way, the support discs of the

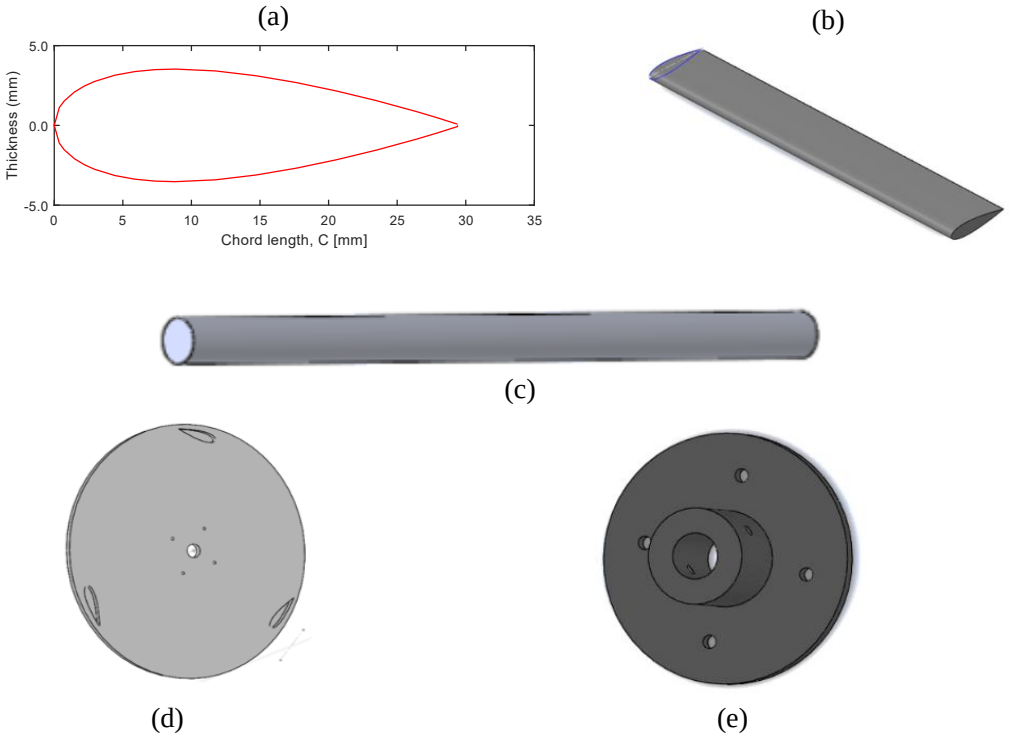

Fig. 4 a) Design of the blade with NACA 0024 configuration with a chord length of 29.4 mm and a length of 210 mm; b) blade profile with NACA 0024 configuration; c) blade support discs of 220 mm in diameter and 5 mm thick; d) 300 mm axis long and 12 mm in diameter; e) Shaft and disc connection hub.

blades of 220 mm in diameter and 5 mm thick are designed, see Fig. 4c. Similarly, the axis of 300 mm in length and 12 mm in diameter is designed, see Fig. 4d. Finally, the hubs for connecting the shaft and discs are designed, which will serve as a fastener between the two components, see Fig. 4e. Last, Fig. S1 shows the assembly of the components made in design software.

2.2 Material and manufacturing method of H-Darrieus wind turbine

The material selected is PETG, which is PET (Polyethylene terephthalate glycol) with carbon fiber reinforcement. This material was selected because it is one of the strongest and toughest filaments available for the fused deposition modeling (FDM) technique, which is an extrusion-based technique for additive manufacturing (AM). Additionally, with these materials, the printed parts will be much lighter and more dimensionally stable than with just the polymer since the fibers prevent the shrinkage of the part as it cools.

The 3D printing parameters for PETG filaments can vary depending on the filament manufacturer, type of 3D printer, and user preferences. However, there are some general settings that are commonly used for printing with PETG:

- The optimal extrusion temperature for PETG is usually in the range of 230 and 250 ℃. This may vary slightly depending on the filament brand and printer.
- The temperature of the heated bed is typically between 80 and 110 ℃ for PETG. This helps prevent warping and promotes better adhesion to the printing surface.
- The recommended printing speed for PETG is generally between 70 and 90 mm/s. A lower speed can help improve print quality and reduce the likelihood of issues such as stringing.
- Some users find it useful to use an adhesion layer such as hairspray or adhesive for PETG prints to improve adhesion to the heated bed.
- Unlike other filaments like PLA, PETG generally requires less ventilation during printing to prevent it from cooling too quickly and causing issues such as delamination.

Table 2 presents some properties of PETG[47] and the parameters utilized for 3D printing turbine blades.

2.3. Assembly and operational tests of the H-Darrieus wind turbine prototype

Once all the components were obtained, the wind turbine was assembled as shown in Fig. S2a. This turbine must be coupled to a test bench which is made of acrylic, which allows it to be connected to a wind tunnel, where several functional tests can be done, see Fig. S2b.

To carry out the tests of the H-Darrieus wind turbine, a

Table 2. 3D Printing parameters for PETG filaments.

Parameter	Value
Density of the filament	1.27 g/cm^3
Molecular weight	300.3706 g/mol
Elongation at break	70%
Tensile strength	26 MPa
Modulus of elasticity	2150 MPa
Melting point	200-230 ˚C
Heat distortion temperature	74 ˚C
Extrusion Temperature	230 ˚C
Temperature of the heated bed	85 ˚C
Printing Speed	80 mm/s

wind tunnel was used to study the effects of airflow. The variables to be measured were torque and rotation speed, thus obtaining the electric power generated and the analysis of the fluctuating torque, very particular for this type of turbines. They also can be optimized to the maximum speed of rotation, with a constant speed of the wind of 6 m/s, where the turbine obtained its highest performance. The articulation of the test bench to the tunnel, the fan motor, the air duct, and the sensor can be seen in Fig. S3.

3. Results and analysis

During the measurements of the power curve, the Futek TRS605 torque sensor with encoder was used coupled to the axis of the wind turbine and a motor with a control system that serves as a load. Sensor data captured was done using the IHH500 Pro display that was connected to the sensor. The data obtained are displayed in Fig. 5, which shows the variation in the power coefficient (C_P) versus the specific or peripheral speed (TSR). This is how the maximum power coefficient generated by the turbine of 0.21 is obtained, equivalent to a 21% efficiency, at a TSR rate of 0.12. When comparing this efficiency with the Betz limit, which stipulates a maximum efficiency in ideal conditions of 59%, the turbine has an appropriate percentage for the type of vertical turbine, which oscillate in efficiencies ranges between 20 and 35% according to the classification carried out by the researchers Beauson *et al*. Thus, the power coefficients according to the type of turbine can be obtained.[48]

This type of Darrieus-type vertical wind turbines normally presents a C_P between 0.2 to 0.4. Although these values are small compared to large horizontal wind turbines with typical values between 0.4 to 0.5, this research work conducted on a laboratory scale presents a significant and acceptable efficiency, able to improve with further research.

The torque variation cycles versus time are summarized in Fig. 6, with the torque variation cycle repeated every second, in an oscillating between 14 to 20 N.mm. This fluctuation is normal in this type of turbines due to its own design, which produces variations according to the position of the blade: the air hits in different ways at the different turning points, causing variations in the force of the air over the turbine, generating the torque variations.

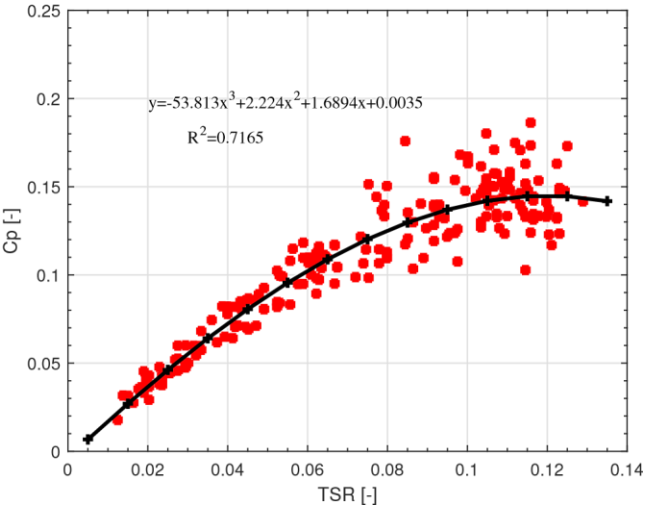

Fig. 5 Power coefficient vs TSR speed for wind turbine.

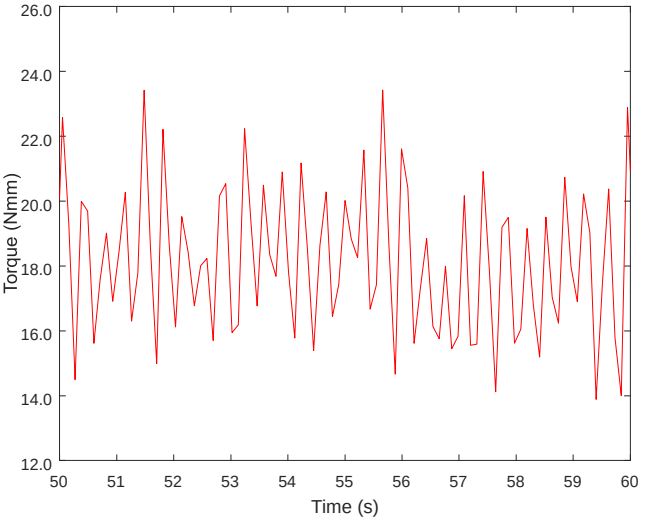

Fig. 6 Torque (Nmm) vs. time (s) for a wind turbine.

4. Life cycle analysis for laboratory scale wind turbine blades

Due to the current environmental questions and needs worldwide, there is a need to understand the impact generated by a product using the concept of life cycle analysis (LCA), which considers all aspects from the extraction to the production of energy and material, the manufacturing, the use, and the final disposal. Thus, the critical points where a considerable environmental load could be generated are identified.[49-51] The NTC-ISO 14040 standard established the procedure for the LCA[52] of a product, going through the

following stages, and shown in Fig. 7.

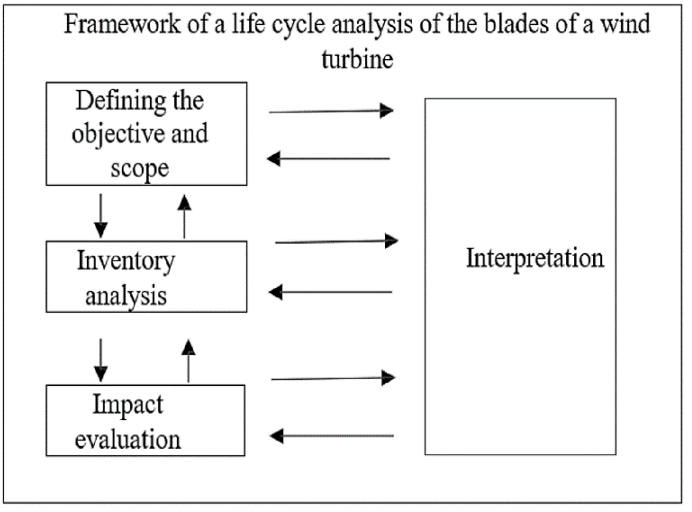

Fig. 7 Stages of life cycle analysis.

The LCA for the wind turbine blades starts by the definition of the objective and scope: it is important to understand the environmental impact generated by the use of 3D printed thermoplastic materials, for the production of blades for an h-Darrieus wind turbine, in order to analyze if this material is less polluting with respect to other materials used for the same purpose. In this way, the wind energy sector could begin to see new ways of manufacturing turbines in a cleaner way for the environment. This follows an inventory analysis: within this stage, it was analyzed the energy and material inputs, the products obtained, and the waste generated during each stage of the process.

- Acquisition of raw materials for the turbine: PET or polyethylene tereph-thalate is one of the most used plastics worldwide. Paraxylene is extracted from petroleum, it is oxidized by air to give way to terephthalic acid, while ethylene is obtained from natural gas, where it is oxidized by air to give way to ethylene glycol. To produce 1 kg of PETG, an average of 1.9 kg of crude oil is used and 23 kWh/kg of electrical energy must be used to produce 1 kg of PETG.[53] For the manufacture of the turbine, 2 kg of PETG were required, and thus a total of 46 kWh/kg were consumed to obtain the raw material. In Colombia, a CO_2 emission factor for electricity generation equivalent to 164.38 g of CO_2 is used for each kilowatt hour (kWh) generated.[54] Therefore, the acquisition of raw material for the manufacture of the blades of the turbine generated 7.56 kg CO_2/kWh.
- Transportation and distribution of the product: because the PETG material was not available in the city of Medellin-Colombia, a request to a company in the city of Bogota-Colombia must be made. Thus, the product had to travel 415 km. On average, a vehicle could consume 9 gallons or 34 L of gasoline to cover this route, since for every 45 km it could consume 1 gallon. According to the research carried out by the Catalan office for climate change, it was established that 2.38 kg of CO_2/L is the carbon footprint for each liter of consumed gasoline. In this way, to transport the material, 80.92 kg of CO_2/L were produced.
- Blade manufacturing process: for the manufacturing process, an FDM type 3D printer was used, which melts the rolled material and extrudes it into a specific shape. The manufacturing time for the 3 blades was 56 h, with a total of 144 g used. According to the technical specifications of the Pegasus MakeR printer, it has a power of 280 Wh, which gives that the electrical consumption was 15.68 kWh, while the value of the carbon footprint in this process is estimated to be 2.57 kg CO_2/kWh.
- Use and maintenance: the blades made with PETG are assembled to the turbine and put into operation to generate energy. An operating time of between 20 and 30 years is estimated, with the turbine generating electricity from the wind and helping to mitigate the carbon footprint for electricity generation. If we assume that the turbine on a laboratory scale works 8 hours a day and produces 0.52 Wh, in 8 hours it will produce 4.16 Wh, in a year it will produce 1.5 kWh, and in 30 years it will produce 45.5 kW. Conver
- ting this data to the amount of CO_2, it is obtained that 7.48 kg CO_2/kWh would be left to be generated into the environment. On the other hand, a periodic preventive maintenance is expected to be carried out on all turbine components that require it.
- Final disposal of process and product waste: PETG is an amorphous thermoplastic, 100% recyclable, so it is possible that after completing its useful life, the turbine can be dismantled to give it a secondary use after a recycling process. A typical process consists of finely grinding the waste generated both during the manufacture and during the dismantling of the turbine, and once the material is ground, it is possible to melt it again to generate new filaments, which could be reused to print new parts. The inputs and outputs of the process for the life cycle analysis of the blades for the H-Darrieus wind turbine are shown in Fig. 8.

The purpose of the environmental impact assessment and LCA of the blades for the H-Darrieus wind turbine is to understand the effects generated in the manufacturing of the blades used in this research. When analyzing the first stage, it was found that during the extraction of oil and the transformation of the components necessary to obtain PETG, 7.56 kg CO_2/kWh were generated due to electricity consumption. Later, in the process of transporting the material,

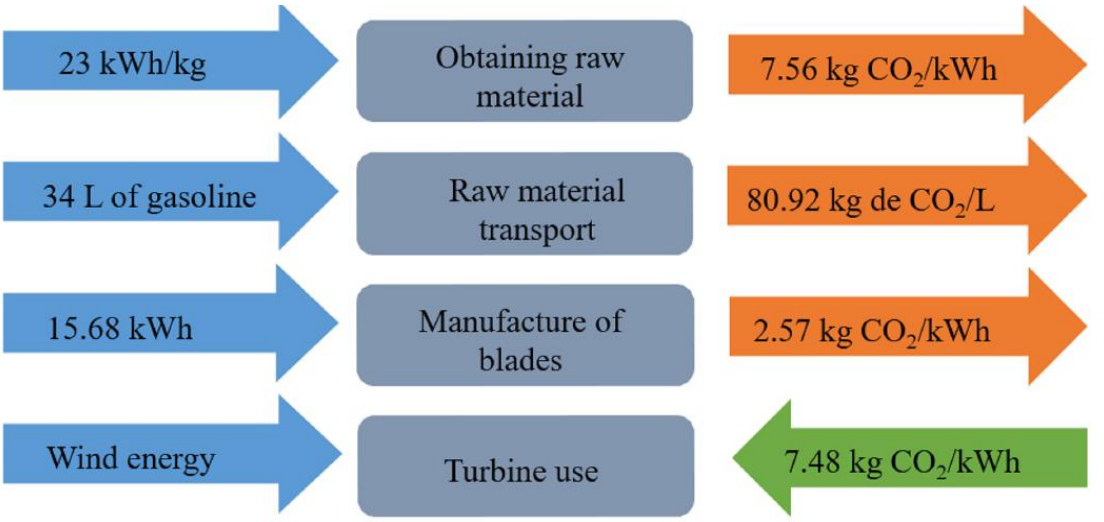

Fig. 8 Inputs and outputs for the life cycle analysis for the followed process.

80.92 kg of CO_2 were generated due to the liters of gasoline used in the transportation process. The value is very high since the combustion of gasoline produces a high CO_2 content in the atmosphere.

Subsequently, in the manufacturing stage of the blades, a carbon footprint of 2.57 kg CO_2/kWh was generated due to the electrical consumption used by the printer for the manufacturing process. Finally, the use of the wind turbine would help to mitigate 7.48 kg CO_2/kWh, leaving a total carbon footprint of 83.57 kg CO_2/kWh. It is important to note that the greatest environmental impact is caused by transportation, which is an indisputable source of contamination. Buying locally would help to reduce this environmental impact by up to 88% of CO_2 emissions into the environment.

5. Conclusions

The current research has shown that manufacturing of the wind turbines is not only feasible as an alternative energy solution but also environmentally and economically sustainable, thus not only having positive impact with the research and development, but also with the environment and local communities. Results could be extended far more beyond the H-Darrieus turbine to many others, basically because the scale, materials, and manufacturing technique are easy to use in many processes.

Additive manufacturing has shown to be a versatile technology for the fabrication of components with complex shapes, and could be further optimized to be more inexpensive, durable, and ecological process, towards optimization via mechanical design and circular economy, a phase of the development that is possible with the scale up for companies in large scale fabrication process. For developing countries, such as Colombia where this research took place, it could represent an opportunity for cutting the gaps in the technology, education, and social development.

The maximum power coefficient obtained was 0.21, at a TSR of 0.12. Looking in the literature for the average C_P for vertical wind turbines, they are in a range of 0.2 and 0.4. Knowing that the maximum mechanical efficiency capable of extracting air from a wind turbine will be 59.3%, can be concluded that the turbine has efficiency within the normal range for its type.

The production of the blades for the H-Darrieus wind turbine generated a carbon footprint of 83.57 kg CO_2/kWh including transportation, and 2.65 kg CO_2/kWh without transportation. The greatest environmental impact occurs in the transport of the raw material of this research, and thus, obtaining the raw materials locally would reduce this effect by up to 88% of CO_2 emissions into the environment, or using other means of transport that do not use energy sources derived from hydrocarbons.

Acknowledgements

The authors gratefully acknowledge the financial support provided by the Colombian Ministry of Science, Technology, and Innovation "MinCiencias" through "Patrimonio Autónomo Fondo Nacional de Financiamiento para la Ciencia, la Tecnología y la Innovación Francisco José de Caldas" (Perseo Alliance, Contract No. 112721-392-2023).

Conflict of Interest

There is no conflict of interest.

Supporting Information

Applicable.

FReferences

[1] M. C. Socci, G. Rodríguez, E. Oliva, S. Fushimi, K. Takabatake, H. Nagatsuka, C. J. Felice, A. P. Rodríguez, Polymeric materials, advances and applications in tissue engineering: a review, *Bioengineering*, 2023, **10**, 218, doi: 10.3390/bioengineering10020218.

[2] J. Zhang, G. Lin, U. Vaidya, H. Wang, Past, present and future prospective of global carbon fibre composite developments and applications, *Composites Part B: Engineering*, 2023, **250**, 110463, doi: 10.1016/j.compositesb.2022.110463.

[3] R. L. B. Cardoso, J. da Silva Rodrigues, R. P. B. Ramos, A. de Castro Correa, E. M. Leão Filha, S. N. Monteiro, A. C. R. da Silva, R. T. Fujiyama, V. S. Candido, Use of yarn and carded jute as epoxy matrix reinforcement for the production of composite materials for application in the wind sector: a preliminary analysis for the manufacture of blades for low-intensity winds, *Polymers*, 2023, **15**, 3682, doi: 10.3390/polym15183682.

[4] S. F. Xavier, Thermoplastic Polymer Composites: Processing, Properties, Performance, Applications and Recyclability. John Wiley & Sons, 2022.

[5] R. Hsissou, R. Seghiri, Z. Benzekri, M. Hilali, M. Rafik, A. Elharfi, Polymer composite materials: a comprehensive review, *Composite Structures*, 2021, **262**, 113640, doi: 10.1016/j.compstruct.2021.113640.

[6] P. K. Penumakala, J. Santo, A. Thomas, A critical review on the fused deposition modeling of thermoplastic polymer composites, *Composites Part B: Engineering*, 2020, **201**, 108336, doi: 10.1016/j.compositesb.2020.108336.

[7] L. Mishnaevsky, K. Branner, H. Petersen, J. Beauson, M. McGugan, B. Sørensen, Materials for wind turbine blades: an overview, *Materials*, 2017, **10**, 1285, doi: 10.3390/ma10111285.

[8] M. A. Abd El-Baky, M. A. Attia, M. M. Abdelhaleem, M. A. Hassan, Flax/basalt/E-glass Fibers Reinforced Epoxy Composites with Enhanced Mechanical Properties, *Journal of Natural Fibers*, 2022, **19**, 954-968, doi: 10.1080/15440478.2020.1775750.

[9] C.-H. Lu, Z.-H. Qi, H. Ge, Y.-L. Zheng, Predicting the mechanical properties of E-glass fiber-reinforced polymer bars after exposure to elevated temperature, *Construction and Building Materials*, 2023, **379**, 131238, doi: 10.1016/j.conbuildmat.2023.131238.

[10] T. Kulhan, A. Kamboj, N. K. Gupta, N. Somani, Fabrication methods of glass fibre composites—a review, *Functional Composites and Structures*, 2022, **4**, 022001, doi: 10.1088/2631-6331/ac6411.

[11] L. Zhang, Q. Y. Zhou, Costing and future development of wind turbine technology, World Scientific Series in Current Energy Issues, *World Scientific*, 2021, 63-84, doi: 10.1142/9789811225925_0003.

[12] A. He, T. Xing, Z. Liang, Y. Luo, Y. Zhang, M. Wang, Z. Huang, J. Bai, L. Wu, Z. Shi, H. Zuo, W. Zhang, F. Chen, W. Xu, Advanced aramid fibrous materials: fundamentals, advances, and beyond, *Advanced Fiber Materials*, 2024, **6**, 3-35, doi: 10.1007/s42765-023-00332-1.

[13] J. Liu, M. Chen, J. Yang, Z. Wu, Study on mechanical properties of basalt fibers superior to E-glass fibers, *Journal of Natural Fibers*, 2022, **19**, 882-894, doi: 10.1080/15440478.2020.1764438.

[14] A. N. Mengal, S. Karuppanan, A. A. Wahab, Basalt carbon hybrid composite for wind turbine rotor blades: a short review, *Advanced Materials Research*, 2014, **970**, 67-73, doi: 10.4028/www.scientific.net/amr.970.67.

[15] N. M. Chikhradze, F. D. S. Marquis, G. S. Abashidze, Hybrid fiber and nanopowder reinforced composites for wind turbine blades, *Journal of Materials Research and Technology*, 2015, **4**, 60-67, doi: 10.1016/j.jmrt.2015.01.002.

[16] Y. Chen, H. Lin, Overview of the development of offshore wind power generation in China, *Sustainable Energy Technologies and Assessments*, 2022, **53**, 102766, doi: 10.1016/j.seta.2022.102766.

[17] A. Vinod, M. R. Sanjay, S. Siengchin, Recently explored natural cellulosic plant fibers 2018–2022: a potential raw material resource for lightweight composites, *Industrial Crops and Products*, 2023, **192**, 116099, doi: 10.1016/j.indcrop.2022.116099.

[18] T. Batu, H. G. Lemu, B. Sirhabizuh, Study of the performance of natural fiber reinforced composites for wind turbine blade applications, *Advances in Science and Technology. Research Journal*. 2020, **14**, 67-75, doi: 10.12913/22998624/118201.

[19] H. Piggot, A wind turbine recipe ebook the axial flux plans metric. Hugh Piggott, Scoraig Wind Electric: Dundonnell, UK, 2014.

[20] A. Diniță, R. G. Ripeanu, C. N. Ilincă, D. Cursaru, D. Matei, R. I. Naim, M. Tănase, A. I. Portoacă, Advancements in fiber-reinforced polymer composites: a comprehensive analysis, *Polymers*, 2023, **16**, 2, doi: 10.3390/polym16010002.

[21] A. Eltayesh, F. Castellani, F. Natili, M. Burlando, A. Khedr, Aerodynamic upgrades of a Darrieus vertical axis small wind turbine, *Energy for Sustainable Development*, 2023, **73**, 126-143, doi: 10.1016/j.esd.2023.01.018.

[22] P. Mohan Kumar, K. Sivalingam, T.-C. Lim, S. Ramakrishna, H. Wei, Review on the evolution of darrieus vertical axis wind turbine: large wind turbines, *Clean Technologies*, 2019, **1**, 205-223, doi: 10.3390/cleantechnol1010014.

[23] W. Zhu, Models for wind tunnel tests based on additive manufacturing technology, *Progress in Aerospace Sciences*, 2019, **110**, 100541, doi: 10.3390/polym16010002.

[24] A. Jandyal, I. Chaturvedi, I. Wazir, A. Raina, M. I. Ul Haq, 3D printing–A review of processes, materials and applications in industry 4.0, *Sustainable Operations and Computers*, 2022, **3**, 33-42, doi: 10.1016/j.susoc.2021.09.004.

[25] H. A. Shah, G. C. Chaudhari, V. D. Dhiman, 3D printed proto type model of pelton turbine runner, *Journal of Physics: Conference Series*, 2023, **2629**, 012002, doi: 10.1088/1742-6596/2629/1/012002.

[26] A. H. Alami, M. Mahmoud, H. Aljaghoub, A. Mdallal, M. Ali Abdelkareem, S. K. Kamarudin, A. G. Olabi, Progress in 3D printing in wind energy and its role in achieving sustainability, *International Journal of Thermofluids*, 2023, **20**, 100496, doi:

10.1016/j.ijft.2023.100496.
[27] S. Arivalagan, R. Sappani, R. Čep, M. S. Kumar, Optimization and experimental investigation of 3D printed micro wind turbine blade made of PLA material, *Materials*, 2023, **16**, 2508, doi: 10.3390/ma16062508.
[28] A. Tarancón, V. Esposito, M. Torrell, M. Di Vece, J. S. Son, P. Norby, S. Bag, P. S. Grant, A. Vogelpoth, S. Linnenbrink, M. Brucki, T. Schopphoven, A. Gasser, E. Persembe, D. Koufou, S. Kuhn, R. Ameloot, X. Hou, K. Engelbrecht, C. R. H. Bahl, N. Pryds, J. Wang, C. Tsouris, E. Miramontes, L. Love, C. Lai, X. Sun, M. R. Kærn, G. Criscuolo, D. B. Pedersen, 2022 roadmap on 3D printing for energy, *Journal of Physics: Energy*, 2022, **4**, 011501, doi: 10.1088/2515-7655/ac483d.
[29] M. Shalby, A. A. Salah, G. A. Matarneh, A. Marashli, M. R. Gommaa, An investigation of a 3D printed micro-wind turbine for residential power production, *International Journal of Renewable Energy Development*, 2023, **12**, 550-559, doi: 10.14710/ijred.2023.52615.
[30] W. Hu, Emerging technologies for next-generation wind turbines. Hu W, Advanced Wind Turbine Technology. Cham: Springer, 2018.
[31] A. Krishnan, A. S. M. Al-Obaidi, L. C. Hao, A comprehensive review of innovative wind turbine airfoil and blade designs: toward enhanced efficiency and sustainability, *Sustainable Energy Technologies and Assessments*, 2023, **60**, 103511, doi: 10.1016/j.seta.2023.103511.
[32] Z. Malecha, G. Dsouza, Modeling of wind turbine interactions and wind farm losses using the velocity-dependent actuator disc model, *Computation*, 2023, **11**, 213, doi: 10.3390/computation11110213.
[33] H. Hou, W. Shi, Y. Xu, Y. Song, Actuator disk theory and blade element momentum theory for the force-driven turbine, *Ocean Engineering*, 2023, **285**, 115488, doi: 10.1016/j.oceaneng.2023.115488.
[34] E. Lenin Chica Arrieta, A. Rubio Clemente, Computational fluid dynamic simulation of vertical axis hydrokinetic turbines. Computational Fluid Dynamics Simulations, IntechOpen, 2020.
[35] R. Vennell, Exceeding the Betz limit with tidal turbines, *Renewable Energy*, 2013, **55**, 277-285, doi: 10.1016/j.renene.2012.12.016.
[36] M. Ragheb, A. M, Wind turbines theory - the betz equation and optimal rotor tip speed ratio. Fundamental and Advanced Topics in Wind Power, InTech, 2011.
[37] K. Tantichukiad, A. Yahya, A. Mohd Mustafah, A. S. Mohd Rafie, A. S. Mat Su, Design evaluation reviews on the savonius, darrieus, and combined savonius-darrieus turbines, *Proceedings of the Institution of Mechanical Engineers, Part A: Journal of Power and Energy*, 2023, 095765092311639, doi: 10.1177/09576509231163965.
[38] S. B. Ray, A. Banerjee, R. Ranjan, T. Maiti, R. Ganguly, Recent advancement in savonius wind turbine- A review, *Journal of Environmental Impact and Management Policy*, 2023, 28-36, doi: 10.55529/jeimp.31.28.36.
[39] M. Ahmadi-Baloutaki, R. Carriveau, D. S.-K. Ting, Straight-bladed vertical axis wind turbine rotor design guide based on aerodynamic performance and loading analysis, *Proceedings of the Institution of Mechanical Engineers, Part A: Journal of Power and Energy*, 2014, **228**, 742-759, doi: 10.1177/0957650914538631.
[40] Y. M. Dai, W. Lam, Numerical study of straight-bladed Darrieus-type tidal turbine, *Proceedings of the Institution of Civil Engineers - Energy*, 2009, **162**, 67-76, doi: 10.1680/ener.2009.162.2.67.
[41] J. Ledoux, S. Riffo, J. Salomon, Analysis of the blade element momentum theory, *SIAM Journal on Applied Mathematics*, 2021, **81**, 2596-2621, doi: 10.1137/20m133542x.
[42] F. Mahmuddin, Rotor blade performance analysis with blade element momentum theory, *Energy Procedia*, 2017, **105**, 1123-1129, doi: 10.1016/j.egypro.2017.03.477.
[43] V. Bhargava, C. Koteshwara Rao, YD Dwivedi, Pressure distribution & aerodynamic characteristics of naca airfoils using computational panel method for 2d lifting flow, *International Journal of Engineering Research*, 2017, **6**, 8–23.
[44] F. Henao, J. P. Viteri, Y. Rodríguez, J. Gómez, I. Dyner, Annual and interannual complementarities of renewable energy sources in Colombia, *Renewable and Sustainable Energy Reviews*, 2020, **134**, 110318, doi: 10.1016/j.rser.2020.110318.
[45] G. Carvajal-Romo, M. Valderrama-Mendoza, D. Rodríguez-Urrego, L. Rodríguez-Urrego, Assessment of solar and wind energy potential in La Guajira, Colombia: current status, and future prospects, *Sustainable Energy Technologies and Assessments*, 2019, **36**, 100531, doi: 10.1016/j.seta.2019.100531.
[46] S. Yagmur, F. Kose, Numerical evolution of unsteady wake characteristics of H-type Darrieus Hydrokinetic Turbine for a hydro farm arrangement, *Applied Ocean Research*, 2021, **110**, 102582, doi: 10.1016/j.apor.2021.102582.
[47] A. Özen, B. E. Abali, C. Völlmecke, J. Gerstel, D. Auhl, Exploring the role of manufacturing parameters on microstructure and mechanical properties in fused deposition modeling (FDM) using PETG, *Applied Composite Materials*, 2021, **28**, 1799-1828, doi: 10.1007/s10443-021-09940-9.
[48] J. Beauson, H. Lilholt, P. Brøndsted, Recycling solid residues recovered from glass fibre-reinforced composites–A review applied to wind turbine blade materials, *Journal of Reinforced Plastics and Composites*, 2014, **33**, 1542-1556, doi: 10.1177/0731684414537131.
[49] Y. F. Nassar, H. J. El-Khozondar, W. El-Osta, S. Mohammed, M. Elnaggar, M. Khaleel, A. Ahmed, A. Alsharif, Carbon footprint and energy life cycle assessment of wind energy industry in Libya, *Energy Conversion and Management*, 2024, **300**, 117846, doi: 10.1016/j.enconman.2023.117846.
[50] A. Schreiber, J. Marx, P. Zapp, Comparative life cycle assessment of electricity generation by different wind turbine types, *Journal of Cleaner Production*, 2019, **233**, 561-572, doi: 10.1016/j.jclepro.2019.06.058.
[51] M. G. Hemeida, A. M. Hemeida, T. Senjyu, D. Osheba, Renewable energy resources technologies and life cycle assessment: review, *Energies*, 2022, **15**, 9417, doi: 10.3390/en15249417.
[52] N. Mir, S. A. Khan, A. Kul, O. Sahin, M. Lachemi, M.

Sahmaran, M. Koç, Life cycle assessment of binary recycled ceramic tile and recycled brick waste-based geopolymers, *Cleaner Materials*, 2022, **5**, 100116, doi: 10.1016/j.clema.2022.100116.
[53] T. Wang, Environmental performance of chair production and distribution in conventional and additive manufacturing. 2023.
[54] D. Duque-Uribe, N. D. Montiel-Bohórquez, J. F. Pérez, Technoeconomic analysis of a small-scale downdraft gasification-based cogeneration power plant using green wastes, *Journal of Energy Resources Technology*, 2023, **145**, 081401, doi: 10.1115/1.4056529.

